Rare Metal Materials and Engineering
Volume 47, Issue 10, October 2018
Online English edition of the Chinese language journal

Available online at www.sciencedirect.com
ScienceDirect

Cite this article as: Rare Metal Materials and Engineering, 2018, 47(10): 3008-3014.

ARTICLE

Electrochemical Performance of a New Type Aluminum Foam/Pb-0.6 wt%Ag Alloy Composite Anode for Zinc Electrowinning Industry

Zhou Xiangyang, Ma Chiyuan, Yang Juan, Wang Shuai, Wang Hui, Long Bo

Central South University, Changsha 410083, China

Abstract: In order to overcome the defects of high over-potential and preparation cost existing in traditional Pb alloy anodes, a new type aluminum foam/Pb-0.6 wt%Ag alloy composite anode (AF/Pb-0.6 wt%Ag anode) was produced. The electrochemical performance of AF/Pb-0.6 wt%Ag anode and traditional Pb-0.6 wt%Ag anode after 72 h galvanostatic polarization in 160 g/L H_2SO_4 solution was investigated comparatively by chronopotentiometry (CP), scanning electron microscopy (SEM), electrochemical impedance spectroscopy (EIS) and Tafel measurements. The results show that the anodic layer of AF/Pb-0.6 wt%Ag anode is more intact than that of the Pb-0.6 wt%Ag anode, and exhibits better corrosion resistance. Moreover, the AF/Pb-0.6 wt%Ag anode shows a lower stable anodic potential, which is consistent with higher PbO_2, lower PbO, $PbO{\cdot}PbSO_4$ content and R_{ct} value obtained by CP and EIS measurements. It is also revealed that the AF/Pb-0.6 wt%Ag anode possesses a better oxygen evolution reaction (OER).

Key words: aluminum foam/Pb-0.6 wt%Ag alloy composite anode; electrochemical performance; anodic layer; corrosion resistance; oxygen evolution reaction

The Pb-(0.25 wt%~1 wt%) Ag alloys have been widely used as insoluble anode materials in the zinc electrowinning industry[1,2]. Although this kind of alloy satisfies the fundamental needs of zinc production, it has several disadvantages[3], such as high anodic over-potential, Pb contamination of the cathode zinc, unsatisfactory mechanical performance, and high consumption of silver. In order to alleviate those problems, researches have been done to produce new type anodes. According to the difference in preparation methods, those research fields can be classified into three aspects in whole: 1) casting way: lead alloy anodes like Pb-Co, Pb-Ca-Sn, Pb-Ag-Sn-Co anodes and Pb-Ag-Nd anode[4-7]; 2) electro-plating coating way: metal coated anodes including Al substrate and Pb substrate, Ti substrate, stainless steel substrate anode like Ti/PbO_2, Al/α-PbO_2-CeO_2-TiO_2/β-PbO_2-WC-ZrO_2, stainlesssteel/β-PbO_2-TiO_2 and Pb/Pb-MnO_2 anode[8-12]; 3) mould-casting way: Al matrix alloy composite anodes like Al/Pb-0.3 wt%Ag alloy composite anode[13].

Among these new-type anodes, the composite Al substrate coated anode and Al matrix alloy anodes get the favour of more and more researchers in recent years due to the good properties of element Al, such as low density, low cost per unit volume, high conductivity and harmless to electrolyte. For example, both Al/Pb-0.3 wt%Ag alloy composite anode and Al/Pb-PANI-WC coated anode[14] show improved anodic behaviors and compact anodic layers. However, how to get an excellent binding between the substrate and the outer alloys (coatings) is still a main problem in efficiently producing those anodes. Although treatments including electro-deposition[10] or pre-plating interlayer (Sn or Pb) on the metal substrate[13] have been adopted to solve this problem, they all make the preparation process lengthy. Besides, the industrial application of the metal coated anode was restricted because of its poor resistance to corrosion and wear. Therefore, it is necessary to explore novel anodes.

In this paper, instead of a Al plate, aluminum foam with

Received date: October 13, 2017
Foundation item: National Nature Science Foundation of China (51304254, 51274240); China Postdoctoral Science Foundation (2015M580698)
Corresponding author: Yang Juan, Ph. D., Associate Professor, School of Metallurgy and Environment, Central South University, Changsha 410083, P. R. China, Tel: 0086-731-88836329, E-mail: jyang_csu@163.com

excellent mechanical properties was used as a substrate to obtain sandwich structural aluminum foam/Pb-0.6 wt%Ag alloy composite anode(AF/Pb-0.6 wt%Ag anode). It is facile for molten Pb-0.6 wt%Ag alloy to flow into the pores of the aluminum foam and form a strong bonding between the two materials. Thus there is no need to pre-plate interlayer or conduct surface pretreatment on the Al substrate. In addition, this method reduces the consumption of silver and the total mass of anode, that is, lower manufacturing cost and possibility of creep deformation. Then the electrochemical performance of AF/Pb-0.6 wt%Ag anode and Pb-0.6 wt%Ag anode was investigated comparatively, including galvanostatic electrolysis, CP, Tafel and EIS measurements. Besides, the microscopic morphologies of the anode metal substrate and the anodized layer polarized for 72 h were obtained by SEM.

1 Experiment

1.1 Preparation of AF/Pb-0.6 wt%Ag anode

The main raw materials used in this experiment were Pb-0.6 wt%Ag alloy (Zhuzhou Smelter Group Co., Ltd) and aluminum foam (Sichuan Yuantaida Group Co., Ltd). The thickness of aluminum foam is 5 mm and the average pore diameter is 2~3 mm.

The entire preparation process included the following steps: 1) The Pb-0.6 wt%Ag alloy was melted in a crucible at 873 K. 2) After the Pb-0.6 wt%Ag alloy was completely melted, the crucible was taken out, and then the aluminum foam was immersed into the molten alloy vertically using a hawkbill. 3) Hawkbill was held for 5 min until the Pb-0.6 wt%Ag alloy was cooled to room temperature in air. 4) The as-obtained AF/Pb-0.6 wt%Ag alloy was wire-cut into cuboids of 10 mm×10 mm×10 mm, with 5 mm-thick aluminum foam in the middle, and a 2.5 mm-thick alloy on the two sides. And the Pb-0.6 wt%Ag alloy was also wire-cut into cuboids of 10 mm×10 mm×10 mm as a contrast sample. 5) The samples were then connected to a plastic-isolated copper wire and cast into a denture base resin with a exposed working area of Pb-0.6 wt%Ag alloy of 1.0 cm^2.

The schematic of preparation process and cross section diagram of AF/Pb-0.6 wt%Ag anode are shown in Fig.1 and Fig.2, respectively.

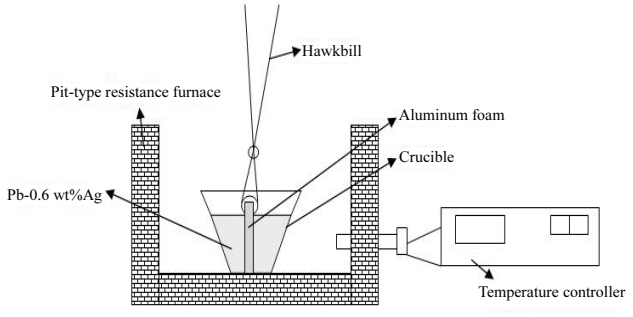

Fig.1 Smelting equipment for the preparation of AF/Pb-0.6 wt%Ag anode

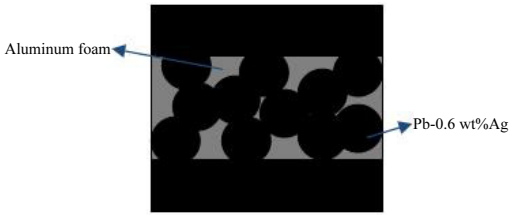

Fig.2 Cross section diagram of AF/Pb-0.6 wt%Ag anode sample

1.2 Measurements

All the electrochemical measurements in this work were conducted with a three-electrode system in a 160 g/L H_2SO_4 solution and the temperature of the test system was controlled at 308 K using a thermostat. A high purity graphite plate (3 cm×3 cm) electrode and Hg/Hg_2SO_4/saturated K_2SO_4 (0.64 V vs standard hydrogen electrode) electrode were employed as the counter electrode and reference electrode, respectively. All potentials in this work were referred to the reference electrode. The working electrodes were gradually ground with SiC sand paper from 400# to 2000# before galvanostatic polarization measurement. Before galvanostatic polarization measurement, the working electrodes were electrolyzed at –500 A/m^2 for 10 min in order to remove the oxides on the anode.

All electrochemical measurements were performed using an electrochemical workstation (PARSTAT 4000, Princeton, USA).

Galvanostatic polarization tests were conducted at 500 A/m^2 in a 160 g/L H_2SO_4 solution for 72 h. An electrochemical workstation was used to record the anodic potential every 60 s. After 72 h galvanostatic polarization, the anodes were subsequently taken out, washed with deionized water, and dried at 333 K for 8 h. Then the morphologies of the anodic layers were observed with environmental scanning electron microscopy (SEM, Quanta FEG 250, Japan). In addition, the morphologies of the metallic substrates were also observed after the anodic layers were removed. The anodic layers were removed by boiling sugar alkali solution (20 g/L glucose and 100 g/L NaOH).

EIS and Tafel measurements were conducted immediately after the stable anodic layer was formed by 72 h galvanostatic polarization. In each EIS measurement, the bias DC potential was set as the anodic potential measured just before the EIS measurement. The amplitude of the AC signal was 10 mV. The frequency range was from 0.1 Hz to 10^5 kHz. The impedance data were fitted to an electrical equivalent circuit (EEC) using the Zsimpwin® program. The best fit was acquired by minimizing χ^2 (Chi squared), which can represent the accuracy of fitting result. The Tafel tests were carried out with a potential ranging from 1.15 V to 1.4 V, and a scanning rate of 0.166 mV/s.

Moreover, CP measurements were carried out after 72 h galvanostatic polarization to identify the phase composition of

the anodic layer. The reduction current was –50 A/m^2 for a duration time of 3 h.

2 Results and Discussion

2.1 Interface microstructure features

Fig.3 shows the interface microstructure morphology between aluminum foam and Pb-0.6 wt%Ag alloy. There are no obvious structural defects around the interfacial bonding region, demonstrating a compact interfacial bonding and strong adhesive strength. Owing to the porosity of oxidation membrane on the aluminum foam, the Pb-0.6 wt%Ag alloy melt can also penetrate into the oxidation layer and form an excellent binding, which is beneficial to the better adhesive strength between aluminum foam and Pb-0.6 wt%Ag alloy. And the excellent binding between aluminum foam and Pb-0.6 wt%Ag alloy contributes to the improved performance of AF/Pb-0.6 wt%Ag anode.

2.2 Galvanostatic polarization

Fig.4 shows the potential-time curves of Pb-0.6 wt%Ag and AF/Pb-0.6 wt%Ag anodes during the galvanostatic polarization for 72 h. At the beginning of the polarization, the anodic potential of the both anodes descends rapidly due to the oxidation reaction of Pb with $PbSO_4$. As the coverage of high-resistance $PbSO_4$ on the anode increases, both anodes tend to have a sustainedly slight decrease owing to the oxidation reaction of $PbSO_4$ with conductive PbO_2. It can be observed that the AF/Pb-0.6 wt%Ag anode takes 50 h to come to a stable state, while the Pb-0.6 wt%Ag anode continues to show a slight decrease trend near the end of galvanostatic polarization. This demonstrates that the AF/Pb-0.6wt% Ag anode is more stable than Pb-0.6wt% Ag anode during galvanostatic polarization process. Besides, the stable anodic potential of the AF/Pb-0.6wt% Ag anode is approximately 10 mV lower than that of the Pb-0.6 wt%Ag anode at the end of galvanostatic polarization, which indicates that the AF/Pb-0.6 wt%Ag anode can facilitate the decrease of anodic potential and energy consumption in the electrolysis process.

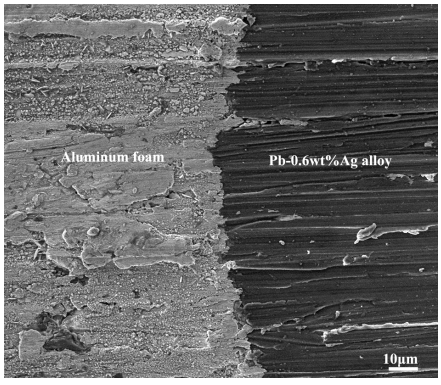

Fig.3 Interface microstructure of AF/Pb-0.6 wt%Ag anode

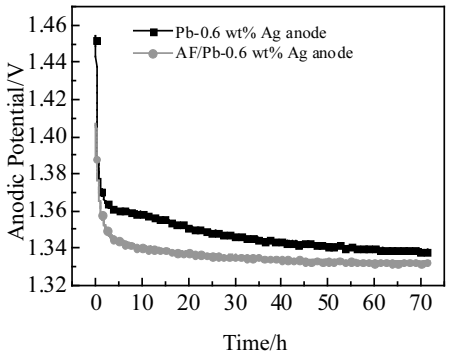

Fig.4 Potential-time curves of Pb-0.6 wt%Ag and AF/Pb-0.6 wt%Ag anodes during the galvanostatic polarization for 72 h

2.3 Morphology of the anodic layer

The surface morphologies of the Pb-0.6 wt%Ag and AF/Pb-0.6 wt%Ag anodes after 72 h galvanostatic polarization are presented in Fig.5. It can be seen that the anodic layer of Pb-0.6 wt%Ag anode in Fig.5a shows a coral-like structure, which is loose and coarse. This can be attributed to the effect of oxygen evolution and the transformation between $PbSO_4$ and PbO_2: the conversion of $PbSO_4$ to PbO_2 results in a 48% decrease in volume, which leads to a porous and incompact passivation film. This kind of structure promotes the contact of electrolyte with Pb alloy substrate, and aggravates the corrosion of the anode. Additionally, these micro-holes can also allow Pb oxides to be easily detached from the anode surface. By comparison, the anodic layer of AF/Pb-0.6 wt%Ag

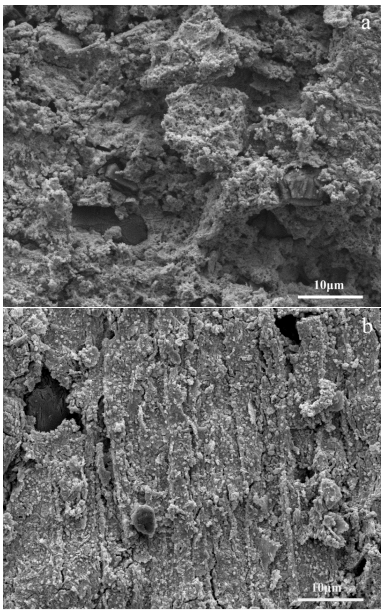

Fig.5 Anodic layers of the Pb-0.6 wt%Ag (a) and AF/Pb-0.6 wt%Ag (b) anode after 72 h galvanostatic polarization

anode shows a flake-like structure and possesses some fine grains, as shown in Fig.5b. And the anodic layer of AF/Pb-0.6 wt%Ag anode is more intact and compact than Pb-0.6 wt%Ag anode and shows a better bonding with substrate in whole. The difference between the two anodes in anodic layer may be related to the sandwich structure of AF/Pb-0.6 wt%Ag anode. And due to the excellent properties of aluminum foam such as high conductivity, low density and strong bonding with Pb-0.6 wt%Ag alloy, it is easier to form a homogeneous anodic layer on the AF/Pb-0.6 wt%Ag anode. Thus it can be concluded that the anodic layer provides a better protection from corrosion for AF/Pb-0.6 wt%Ag anode and helps to prolong the anode service life.

2.4 Morphology of the metallic substrate

In order to analyze the corrosion resistance between the two anodes, the metallic morphologies of them after 72 h galvanostatic polarization are exhibited in Fig.6. It turns out that the substrate corrosion for both anodes occurs preferentially around the interdendritic boundaries, which is called a chemically active region. The both anodes undergo homogeneous corrosion and show corrosion cracks and micro-holes at the interdendritic boundaries. However, the Pb-0.6 wt%Ag anode in Fig.6a exhibits more corrosion cracks and deeper micro-holes than AF/Pb-0.6 wt%Ag anode in Fig.6b, indicating that the Pb-0.6 wt%Ag anode suffers more severe corrosion. This may be due to the following factors: the anodic layer of the AF/Pb-0.6 wt%Ag anode is thicker and tightly bound to the metallic substrate, which alleviates the substrate corrosion. It can be concluded that the corrosion behavior is consistent with the discussion of the morphology of the anodic layer mentioned in section 2.3, and the AF/Pb-0.6 wt%Ag anode shows a better corrosion resistance.

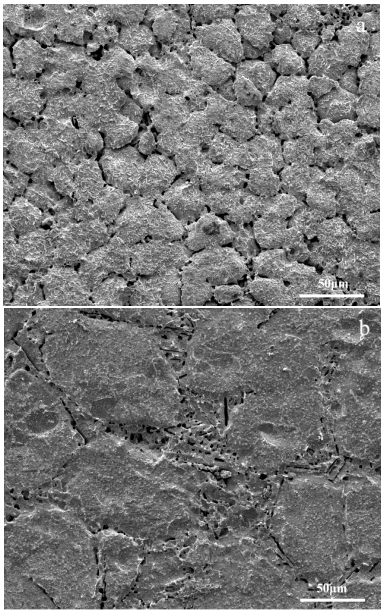

Fig.6 Morphologies of metallic substrate of the Pb-0.6 wt%Ag (a) and AF/Pb-0.6 wt%Ag (b) anode after 72 h galvanostatic polarization

2.5 CP measurement

CP measurement was adopted to identify the composition and concentration of the formed anodic layer. After 72 h galvanostatic polarization with a current density of 500 A/m^2, the reduction current of –5 mA/cm^2 was applied to the two anodes. Then the high valence oxide of anodic layers is reduced to the low valence oxide successively, and the relevant potential platform is exhibited in Fig.7. The length of each potential platform can represent the electric quantity needed for the reduction of relevant Pb oxide, that is, the concentration of the oxides.

It can be seen from Fig.7 that there are four obvious potential platforms for each anode. The platform I, at about –0.9 V, signifies the reduction of PbO_2. The transformation can be expressed by Eq.(1).

$$PbO_2+2e+4H^+ \rightarrow Pb^{2+}+2H_2O \quad (1)$$

And the platform II, at about –1.2 V, signifies the reduction of PbO, PbO_n (PbO and tetra-PbO_n), and a small amount of basic lead sulfate. These transformations can be expressed by Eqs.(2~4).

$$PbO+PbSO_4+4e+2H^+ \rightarrow 2Pb+SO_4^{2-}+H_2O \quad (2)$$

$$3PbO\cdot PbSO_4\cdot H_2O+8e+6H^+ \rightarrow 4Pb+SO_4^{2-}+4H_2 \quad (3)$$

$$PbO_2+2e+2H^+ \rightarrow Pb+H_2O \quad (4)$$

At a more negative potential, platform III appears, corresponding to the reduction of $PbSO_4$ to sponge Pb. The transformation can be expressed by Eq.(5).

$$PbSO_4+2e \rightarrow Pb+SO_4^{2} \quad (5)$$

In addition, at about –1.4V, platform IV appears, representing the evolution of H_2.

The reduction electric quantity can be calculated by the following formula:

$$Q_i=IA(t_{i+1}-t_i) \quad (6)$$

where Q_i represents the reduction electric quantity of the platform i(i=I, II, III) (C); I represents current density of reduction (A/m^2); A represents anode's area (m^2); t_i is the

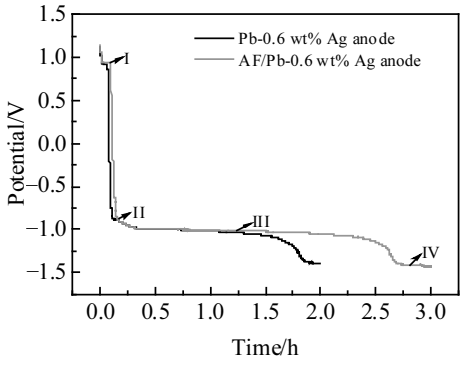

Fig.7 CP curves of Pb-0.6 wt%Ag anode and AF/Pb-0.6 wt%Ag anode

starting time of platform *i*.

Therefore, Table 1 was obtained through the formula above.

Table 1 shows the reduction electric quantity of each platform. Both the anodic layers mainly consist of PbO_2, $PbSO_4$, non-stoichiometric PbO and $PbO{\cdot}PbSO_4$. And it is obvious that the total reduction electric quantity of the AF/Pb-0.6wt%Ag anode is higher than that of Pb-0.6 wt%Ag anode, so it can be concluded that anodic layer of the former is thicker than the latter, which also explains the better corrosion resistance of AF/Pb-0.6 wt%Ag anode. In addition, the AF/Pb-0.6 wt%Ag anode shows a lower content of PbO and $PbO{\cdot}PbSO_4$, which contributes to the decrease of the anodic layer impedance and explains the lower anodic potential of the AF/Pb-0.6 wt%Ag anode.

Owing to the lower $PbO{\cdot}PbSO_4$ content and higher total reduction electric quantity, the AF/Pb-0.6 wt%Ag anode presents a thicker anodic layer and a lower anodic potential. This indicates that the AF/Pb-0.6 wt%Ag anode has a great potential on energy-saving.

2.6 Oxygen evolution behavior

As the conclusions of previous study, the over-potential of OER critically takes a great part in the energy consumption during the zinc electrowinning. Therefore, the oxygen evolution behaviors of the two anodes were investigated in this paper.

2.6.1 AC impedance

EIS measurement is an effective way to investigate OER on the stable anodic layer of metallic oxide electrodes[15,16]. Fig.8 shows the Nyquist plots of Pb-0.6 wt%Ag anode and AF/Pb-0.6 wt%Ag anode after 72 h polarization. It is obvious that only one capacitance arc appears in the Nyquist pattern, which reveals that the charge transfer resistance of OER is in parallel with the double layer capacitance. In addition, an obvious inductance L is observed in the high frequency region, which can be classified as the charge relaxation of electro-active materials containing heterogeneity or energy disorder[17]. The electrical equivalent circuit (EEC) in Fig.9 was used to fit the EIS data. R_u represents the electrolyte resistance between the reference electrode and the working electrode, and R_{ct} represents the charge-transfer resistance in the electrochemical process. The use of a constant phase element (CPE) is a good approach to study the solid electrodes with different surface roughness, physical nonuniformity or uneven distribution of surface reaction sites[18,19]. The impedance of CPE can be expressed as:

$$Z_{CPE}=\frac{1}{Q(j\omega)^n} \quad (7)$$

Table 1 Reduction electric quantity of each platform (C)

Anode	PbO_2	PbO and $PbO{\cdot}PbSO_4$	$PbSO_4$	Total electric quantity
Pb-0.6 wt%Ag	1.295	2.07	27.895	31.26
AF/Pb-0.6 wt%Ag	1.78	1.585	41.405	44.77

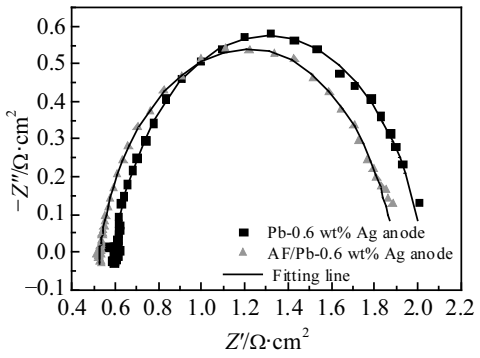

Fig.8 Nyquist plots of Pb-0.6 wt%Ag anode and AF/Pb-0.6 wt%Ag anode after 72 h polarization

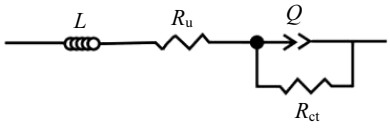

Fig.9 Electrical equivalent circuit

where Q is the capacity parameter ($F{\cdot}cm^{-2}{\cdot}s^{n-1}$), ω is the angular frequency, and n represents the deviation from the ideal behavior (n is 1 for the perfect capacitance). Brug et al[18] proposed that the C_{dl} is associated with the uncompensated resistance R_u and the charge transfer resistance R_{ct}, as expressed as:

$$Q=(C_{dl})^n[(R_u)^{-1}+(R_{ct})^{-1}]^{(1-n)} \quad (8)$$

Thus, C_{dl} was calculated using the Q obtained from the EEC fitting. The simulated patterns and the parameters obtained through EEC fitting are shown in Fig.8 (lines) and Table 2, respectively.

As shown in Table 2, the λ^2 values of EEC fitting of both anodes are around 10^{-4}, suggesting that the simulation results meet the required precision. The AF/Pb-0.6 wt%Ag anode presents a higher double layer capacity (C_{dl}). This indicates that more charged species are absorbed at the anodic layer/electrolyte interface during the polarization process of the AF/Pb-0.6 wt%Ag anode[9]. And the Q value of AF/Pb- 0.6 wt% Ag anode is higher than that of the Pb-0.6 wt%Ag

Table 2 Equivalent circuit parameters for the Pb-0.6 wt%Ag and AF/Pb-0.6 wt%Ag anodes

Parameter	Pb-0.6 wt%Ag	AF/Pb-0.6 wt%Ag
$L/\times10^{-7}$ H·cm²	2.661	3.396
Q/F·cm^{-2}·s^{n-1}	0.0638	0.0701
$C_{dl}/\times10^{-2}$ F·cm^{-2}	3.65	3.74
$R_u/\Omega{\cdot}cm^2$	0.5953	0.5266
$R_{ct}/\Omega{\cdot}cm^2$	1.425	1.366
n	0.8663	0.8520
$\lambda^2/\times10^{-4}$	2.857	1.432

anode, which demonstrates that the former has higher electrocatalytic activity than the latter.

In addition, the smaller R_{ct}, corresponding to the smaller capacitive loop in the pattern of the polarized AF/Pb-0.6 wt%Ag anode may be related to the higher concentration of PbO_2, which is proved by the CP analysis in section 2.5. According to the OER mechanism proposed by Clancy[1], PbO_2 is an essential factor for the generation of OER zones. Thus a higher concentration of PbO_2 helps to form a larger number of reaction sites for OER. Consequently, the polarized AF/Pb-0.6 wt%Ag anode presents a lower anodic potential. In summary, the higher C_{dl} value and lower R_{ct} value indicate that it is easier for OER to proceed on the surface of AF/Pb-0.6 wt%Ag anode.

2.6.2 Tafel analysis

The following reaction steps have been proposed as the mechanism for oxygen evolution after the stable anodic layer formed on active metal oxide electrodes[20-22]:

$$S+H_2O \rightarrow S{\cdot}OH_{ads}+H^+ +e \quad (9)$$

$$S{\cdot}OH_{ads} \rightarrow S{\cdot}O_{ads}+H^+ +e \quad (10a)$$

$$2S{\cdot}OH_{ads} \rightarrow S{\cdot}O_{ads}+S+H_2O \quad (10b)$$

$$2S{\cdot}O_{ads} \rightarrow 2S+O_2 \quad (11)$$

where S represents the active sites on the anode surface and $S\text{-}OH_{ads}$, $S\text{-}O_{ads}$ is the adsorbed intermediates. Among the three steps, the rate determining step for a specific electrode is normally related to its Tafel slope for oxygen evolution, because the Tafel slope depends on the type, composition and physical properties of the oxide electrodes[20,23]. For the lead dioxide electrode, it is concluded that when the Tafel slope b, is ≥120 mV/dec, Eq.(10a) is rate determining step; when b is ~40 mV/dec, Eq. (10b) is rate determining step; when the Tafel slope is ~15 mV/dec, the rate determining step is Eq. (11)[19,24].

In this paper, the corrected over potential (η) is used to represent the real potential of the oxygen evolution. The anodic polarization curve of the Tafel analysis was corrected by Eq. (12):

$$\eta = E_{appl} - iR + 0.64\ V - 1.25\ V \quad (12)$$

where E_{appl} is the applied potential, i is the Faraday current, 0.64 V is the potential of mercury sulfate electrodes, and 1.25 V is the reversible potential of oxygen evolution calculated by the Nernst equation in a synthetic zinc electrowinning electrolyte of 160 g/L H_2SO_4 at 308 K[14], and R is the electrolyte resistance and it can be approximated by the R_u values exhibited in Table 2.

The results shown in Fig.10 and Table 3 are obtained via potential sweep from 1.15 V to 1.4 V after 72 h polarization. After the ohmic-drop correction, Tafel lines of the two anodes present two distinct linear segments in both the low potential region and the high potential region. In low over-potential regions, the Tafel slopes b_1 of Pb-0.6 wt%Ag anode and AF/Pb-0.6 wt%Ag anode are 124 and 115 mV/dec, respectively. And the lower slope value of AF/Pb-0.6 wt%Ag anode may be related to the lower R_{ct} value of the AF/Pb-0.6 wt%Ag anode calculated in section 2.6.1. In high over-potential regions, the Tafel slopes b_2 of Pb-0.6 wt%Ag anode and AF/Pb-0.6 wt%Ag anode, increase to 160 and 170 mV/dec, respectively. Both Tafel slopes increase to some extent, and some studies have attributed the increase in the slope value to the influence of partially evolved O_3[19]. According to the principles mentioned above, the formation and adsorption of OER intermediates is suggested to be the rate determination step for both anodes. Furthermore, the Tafel slope of the AF/Pb-0.6 wt%Ag anode is slightly larger than that of Pb-0.6 wt%Ag anode in the high potential region. This is probably because the structure of AF/Pb-0.6 wt%Ag anode is more favorable for the evolution of O_3[10]. In industrial practice, the applied current density is 0.05 A/cm^2, which is located in the high over-potential region. Therefore, the over-potential values of the two anodes can be calculated using Tafel formula parameters for this region. The result is listed in Table 3. It can be concluded that the over-potential of AF/Pb-0.6 wt%Ag anode is about 15 mV lower than that of the Pb-0.6 wt%Ag anode, demonstrating that its anodic layer is preferable to OER and energy-saving. This result is also consistent with the lower anodic potential of AF/Pb-0.6 wt%Ag anode.

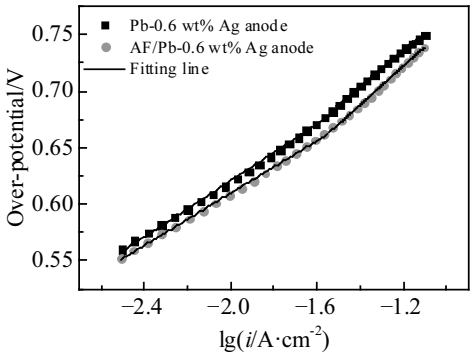

Fig.10 Tafel curves of Pb-0.6 wt%Ag anode and AF/Pb-0.6 wt%Ag anode

Table 3 OER dynamic parameters of Pb-0.6 wt%Ag anode and AF/Pb-0.6 wt%Ag anodes obtained from the Tafel lines in Fig.10

Anode	b_1/mV·dec^{-1}	b_2/mV·dec^{-1}	η(i=0.05 A·cm^{-2})/V
Pb-0.6 wt%Ag	124	160	0.720
AF/Pb-0.6 wt%Ag	115	170	0.705

3 Conclusions

1) The AF/Pb-0.6 wt%Ag alloy composite anode shows a lower anodic potential than the Pb-0.6 wt%Ag anode. This may be related to the higher content of PbO_2 and the lower content of PbO_n on the anodic layer of AF/Pb-0.6 wt%Ag anode.

2) Compared with Pb-0.6 wt%Ag anode, the anodic layer of

AF/Pb-0.6 wt%Ag anode has a flake-like structure with some fine grains on it. Owing to the thicker anodic layer and stronger binding force with substrate, the AF/Pb-0.6 wt%Ag anode exhibits better corrosion resistance.

3) The Pb-0.6 wt%Ag anode and AF/Pb-0.6 wt%Ag anode exhibit a common kinetic mechanism, and the OER of the two anodes is exclusively controlled by the formation and adsorption of intermediate. And the lower R_{ct} value further explains the lower anodic potential of Pb-0.6 wt%Ag anode.

4) In the high potential region corresponding to the industry applied current density, the AF/Pb-0.6 wt%Ag anode has a lower over-potential than the industrial Pb-0.6 wt%Ag, which is advantageous for energy-saving.

References

1 Clancy M, Bettles C J, Stuart A *et al*. *Hydrometallurgy*[J], 2013, 131: 144

2 Felder A, Prengaman R D. *JOM: the Journal of the Minerals Metals & Materials Society*[J], 2006, 58(10): 28

3 Lai Y Q, Jiang L X, Li J *et al*. *Hydrometallurgy*[J], 2010, 102(1): 73

4 Ivanov I, Stefanov Y, Noncheva Z *et al*. *Hydrometallurgy*[J], 2005, 7(2): 109

5 Rashkov S, Dobrev T, Noncheva Z *et al*. *Hydrometallurgy*[J], 1999, 52(3): 223

6 Rashkov S, Stefanov Y, Noncheva Z *et al*. *Hydrometallurgy*[J], 1996, 40(3): 319

7 Zhong X C, Gui J F, Yu X Y *et al*. *Acta Physico-Chimica Sinica*[J], 2014, 30(3): 492

8 Chen B M, Guo Z C, Huang H *et al*. *Acta Metallurgica Sinica-English Letters*[J], 2009, 22(5): 373

9 Lai Y Q, Li Y, Jiang L X *et al*. *Journal of Electroanalytical Chemistry*[J], 2012, 671: 16

10 Li Y, Jiang L X, Lv X J *et al*. *Hydrometallurgy*[J], 2011, 109(3-4): 252

11 Song Y C, Wei G, Xiong R C *et al*. *Electrochimica Acta*[J], 2007, 52(24): 7022

12 Stefanov Y, Dobrev T. *Transactions of the Institute of Metal Finishing*[J], 2005, 83(6): 296

13 Yang H T, Liu H R, Zhang Y C *et al*. *International Journal of Minerals Metallurgy and Materials*[J], 2013, 20(10): 56

14 Xu R D, Huang L P, Zhou J F *et al*. *Hydrometallurgy*[J], 2012, 125: 8

15 Yang C J, Ko Y, Park S M. *Electrochimica Acta*[J], 2012, 78: 615

16 Zhang W, Houlachi G. *Hydrometallurgy*[J], 2010, 104(2): 129

17 Bisquert J, Randriamahazaka H, Garcia-Belmonte G. *Electrochimica Acta*[J], 2005, 51(4): 627

18 Brug G J, Eeden A L G V D, Sluyters-Rehbach M *et al*. *Journal of Electroanalytical Chemistry*[J], 1984, 176(1): 275

19 Franco D V, Da Silva L M , Jardim W F *et al*. *Journal of the Brazilian Chemical Society*[J], 2006, 17(4): 746

20 Aromaa J, Forsen O. *Electrochimica Acta*[J], 2006, 51(27): 6104

21 Shrinastava P, Moats M S. *Journal of Applied Electrochemistry* [J], 2009, 39(1): 107

22 Silval M D, Boodts J F C, Farials A D. *Electrochimica Acta*[J], 2001, 46(9): 1369

23 Morimitsu M, Otogawa R, Matsunaga M. *Electrochimica Acta*[J], 2000, 46(2): 401

24 Silva L M D, De Farials L A, Boodts J F C. *Pure & Applied Chemistry*[J], 2001, 73(12): 1871

锌电积工业用新型泡沫铝/Pb-0.6%Ag 合金复合阳极的电化学性能

周向阳，马驰原，杨　娟，王　帅，王　辉，龙　波

(中南大学，湖南 长沙 410083)

摘　要：为克服传统锌电积阳极存在的高析氧过电位和高银含量的缺陷，发明了一种新型泡沫铝/Pb-0.6% Ag（质量分数）复合阳极。采用计时电位法，扫描电镜，交流阻抗法和塔菲尔测试法对比研究了在 160 g/L H_2SO_4 溶液中极化 72 h 后泡沫铝/Pb-0.6% Ag 复合阳极和 Pb-0.6% Ag 阳极的电化学性能。结果表明：泡沫铝/Pb-0.6% Ag 复合阳极的阳极膜比 Pb-0.6% Ag 阳极的更平整，且抗腐蚀能力更强。此外，泡沫铝/Pb-0.6% Ag 复合阳极的稳定阳极电位更小，与通过计时电位法和交流阻抗法获得的高 PbO_2，低 PbO, $PbO{\cdot}PbSO_4$ 含量和低 R_{ct} 值一致。泡沫铝/Pb-0.6% Ag 复合阳极具有更优异的析氧反应行为。

关键词：泡沫铝/Pb-0.6% Ag 复合阳极；电化学性能；阳极膜； 耐腐蚀性； 析氧反应

作者简介：周向阳，男，1969 年生，博士，教授，中南大学冶金与环境学院，湖南 长沙 410083，电话：0731-88836329，E-mail: xyzhou_csu@163.com